Measuring mechanical motion with a single spin

2012 New J. Phys. 14 125004

(http://iopscience.iop.org/1367-2630/14/12/125004)

New Journal of Physics
The open access journal for physics

Measuring mechanical motion with a single spin

S D Bennett[1,5], S Kolkowitz[1], Q P Unterreithmeier[1], P Rabl[2], A C Bleszynski Jayich[3], J G E Harris[4] and M D Lukin[1]

[1] Department of Physics, Harvard University, Cambridge, MA 02138, USA
[2] Institute for Quantum Optics and Quantum Information of the Austrian Academy of Science, A-6020 Innsbruck, Austria
[3] Department of Physics, University of California Santa Barbara, Santa Barbara, CA 93106, USA
[4] Departments of Physics and Applied Physics, Yale University, New Haven, CT 06520, USA
E-mail: bennett@physics.harvard.edu

New Journal of Physics **14** (2012) 125004 (17pp)
Received 30 May 2012
Published 10 December 2012
Online at http://www.njp.org/
doi:10.1088/1367-2630/14/12/125004

Abstract. We study theoretically the measurement of a mechanical oscillator using a single two-level system as a detector. In a recent experiment, we used a single electronic spin associated with a nitrogen–vacancy center in diamond to probe the thermal motion of a magnetized cantilever at room temperature (Kolkowitz *et al* 2012 *Science* **335** 1603). Here, we present a detailed analysis of the sensitivity limits of this technique, as well as the possibility to measure the zero-point motion of the oscillator. Further, we discuss the issue of measurement backaction in sequential measurements and find that although backaction heating can occur, it does not prohibit the detection of zero-point motion. Throughout the paper, we focus on the experimental implementation of a nitrogen–vacancy center coupled to a magnetic cantilever; however, our results are applicable to a wide class of spin–oscillator systems. The implications for the preparation of nonclassical states of a mechanical oscillator are also discussed.

[5] Author to whom any correspondence should be addressed.

Contents

1. Introduction

Recent interest in mechanical oscillators coupled to quantum systems is motivated by quantum device applications and by the goal of observing the quantum behavior of macroscopic mechanical objects. The last decade has seen rapid progress in studying mechanical oscillators coupled to quantum two-level systems such as superconducting qubits [1–3] and single electronic spins [4], and theoretical work has explored strong mechanical coupling to collective atomic spins [5–7]. Recently, it was proposed that a mechanical oscillator could be strongly coupled to an individual spin qubit [8, 9]. Experiments based on single spins coupled to mechanical systems have demonstrated scanning magnetometry [10], mechanical spin control [11] and detection of mechanical motion [12, 13]. In parallel, pulsed spin control techniques have attracted renewed interest in decoupling a spin from the low-frequency noise in its environment, extending its coherence [14] while also enhancing the sensitivity of the spin to magnetometry [15–18].

In this paper, we consider pulsed single spin measurements applied to the detection of mechanical motion at the single phonon level. We extend the analysis presented in our recent work [13], providing a detailed theoretical framework and a discussion of measurement backaction. The central concept of our measurement approach is to apply a sequence of control pulses to the spin, synchronizing its dynamics with the period of a magnetized cantilever, thereby enhancing its sensitivity to the motion. By measuring the variance of the accumulated phase imprinted on the spin by the oscillator during a measurement, we directly probe the average phonon number, despite the fact that the oscillator position is linearly coupled to

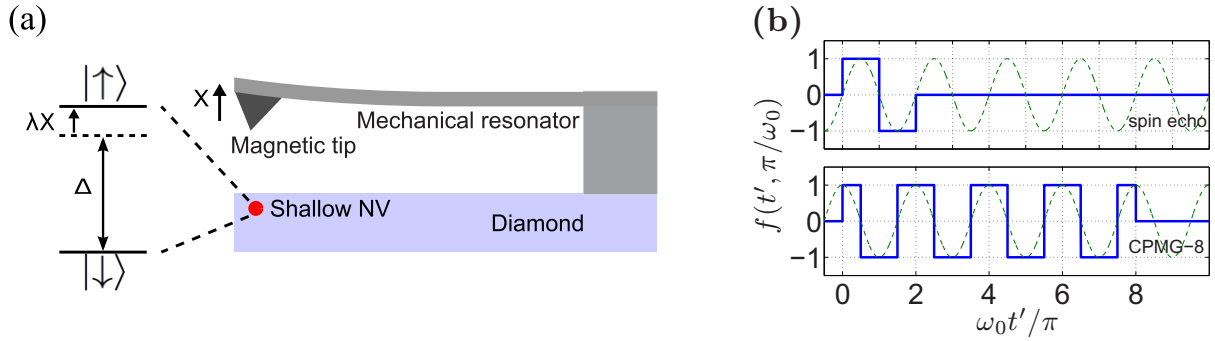

Figure 1. (a) Schematic diagram of the setup. A single spin can be used to measure mechanical motion via magnetic coupling. (b) Toggling sign of the interaction describing π pulses flipping the spin. Each sequence begins and ends with $\pi/2$ pulses, and π pulses flip the sign of the interaction at regular intervals of time τ. The thin dashed line shows the oscillator position, which is synchronized with the pulse sequence for $\tau = \pi/\omega_0$ as shown. The total sequence time is $t = 2\tau$ for spin echo and $t = N\tau$ for CPMG.

the transition frequency of the spin. We derive the conditions for observing a single phonon using the spin as a detector, and find that these conditions coincide with that of large effective cooperativity, sufficient to perform a two-spin gate mediated by mechanical motion [19]. Further, we consider the backaction arising from sequential measurements and show that this does not prohibit single phonon resolution. Throughout the paper, we focus on the specific spin–oscillator system of a magnetized cantilever coupled to the electronic spin associated with a nitrogen–vacancy (NV) center in diamond. For realistic experimental parameters, we find that this system can reach the regime of large cooperative spin–phonon coupling, and the spin may be used to measure and manipulate mechanical motion at the quantum level.

We begin in section 2 by introducing the coupled system and spin control sequences, and calculate the signal due to thermal and driven motion of the oscillator. Then in section 3 we derive the optimal phonon number sensitivity, and show the relation between strong cooperativity and single phonon resolution. Finally, in section 4, we consider the limit of zero temperature and calculate the signal due to zero-point motion, including a discussion of backaction heating for sequential measurements.

2. Coherent sensing of mechanical motion

2.1. The model

We consider the setup shown schematically in figure 1, in which a magnetized cantilever is coupled to the electronic spin of a single NV center. The magnetic tip generates a field gradient at the location of the NV, and as a result its motion modulates the magnetic field seen by the spin causing Zeeman shifts of its precession frequency. To lowest order in small cantilever motion, the precession frequency depends linearly on the position of the tip and is described by the Hamiltonian ($\hbar = 1$)

$$\hat{H} = \frac{\Delta}{2}\hat{\sigma}_z + \frac{\lambda}{2}\left(\hat{a} + \hat{a}^\dagger\right)\hat{\sigma}_z + \hat{H}_{\rm osc}, \tag{1}$$

where $\hat{\sigma}_z$ is the Pauli operator of the spin and $\hat{a}$ is the annihilation operator of the oscillator. For a spin associated with an NV center in diamond, we take $|\uparrow\rangle = |m_s = 1\rangle$ and $|\downarrow\rangle = |m_s = 0\rangle$ in the spin-1 ground state of the NV center, and safely ignore the $|m_s = -1\rangle$ state assuming that it is far detuned by an applied dc magnetic field. Δ is the detuning of the microwave pulses used for spin manipulation, which plays no role in what follows, and we take $\Delta = 0$ throughout the paper. The spin–oscillator coupling strength is $\lambda = g_e \mu_B G_m x_0/\hbar$, where $g_e \approx 2$ is the Landé g-factor, μ_B is the Bohr magneton, G_m is the magnetic field gradient along the NV axis and $x_0 = \sqrt{\hbar/2m\omega_0}$ is the zero-point motion of the cantilever mode of mass m and frequency ω_0 (we included $\hbar$ in the definitions of λ and x_0 for clarity). The damped, driven oscillator is described by

$$\hat{H}_{osc} = \omega_0 \hat{a}^\dagger \hat{a} + \hat{H}_\gamma + \hat{H}_{dr}, \tag{2}$$

where

$$\hat{H}_\gamma = \sum_k g_k (\hat{a} + \hat{a}^\dagger)(\hat{b}_k + \hat{b}_k^\dagger) + \sum_k \omega_k \hat{b}_k^\dagger \hat{b}_k \tag{3}$$

describes the dissipative coupling to a bath of oscillators $\hat{b}_k$, characterized by damping rate γ and temperature T. Finally, $\hat{H}_{dr}$ describes a coherent oscillator drive which we consider briefly in section 2.4. Note that in equation (1) we have temporarily omitted the intrinsic spin decoherence due to the environment; we will include this explicitly in section 3.

2.2. *Spin echo and multipulse sequences*

The motion of the oscillator imprints a phase on the spin as it evolves under equation (1), which can be detected using spin echo [3, 20], or more generally a multiple pulse measurement. Throughout the paper, we focus on Carr–Purcell–Meiboom–Gill (CPMG)-type pulse sequences, consisting of equally spaced π pulses at intervals of time τ, as depicted in figure 1. After initialization in $|\uparrow\rangle$, a $\pi/2$ pulse prepares the spin in an eigenstate of $\hat{\sigma}_x$, $|\psi_0\rangle = \frac{1}{2}(|\uparrow\rangle + |\downarrow\rangle)$ with $\langle\psi_0|\,\hat{\sigma}_x\,|\psi_0\rangle = 1$. The spin is then allowed to interact with the oscillator for time t, accumulating a phase, during which time we apply a sequence of π pulses that effectively reverse the direction of spin precession. At the end of the sequence, a final $\pi/2$ pulse converts the accumulated phase into a population in $|\uparrow\rangle$, which is then read out. By applying both the initial and final $\pi/2$ rotations about the same axis, we measure the probability to find the spin in its initial state $|\psi_0\rangle$ at the end of the sequence, given by

$$P(t) = \tfrac{1}{2}(1 + \langle\hat{\sigma}_x(t)\rangle), \tag{4}$$

where the angle brackets denote the average over spin and oscillator degrees of freedom. Our choice to measure $\hat{\sigma}_x$ probes the accumulated phase variance; this is crucial for our purpose because the average phase imprinted by an undriven fluctuating oscillator is zero. In contrast, by applying the first and final $\pi/2$ pulses about the orthogonal axes, one would instead measure $\hat{\sigma}_y$, which probes the average accumulated phase. This difference can be seen from equation (1) in the absence of the oscillator, in which case $\langle\hat{\sigma}_x(t)\rangle = \cos\Delta t$, whereas $\langle\hat{\sigma}_y(t)\rangle = \sin\Delta t$, which are, respectively, quadratic and linear in a small accumulated phase Δt.

The sensitivity of the spin to mechanical motion is determined by the impact of the oscillator on the spin coherence $\langle\hat{\sigma}_x(t)\rangle$. The key to maximizing this impact is to synchronize the spin evolution with the mechanical period using a CPMG sequence of π pulses, increasing the accumulated phase variance and improving the sensitivity as discussed in the context of ac magnetometry [21]. Choosing $\tau = \pi/\omega_0$ between the π pulses, we flip the spin every half-period

of the oscillator and maximize the accumulated phase variance. At the same time, these pulse sequences decouple the spin from low-frequency magnetic noise of the environment, extending the spin coherence time T_2 [16, 17]. We describe the effects of the applied π pulses using a function $f(t,\tau)$, which flips the sign of the spin–oscillator interaction at regular intervals of time τ as illustrated in figure 1. In this toggling frame, the interaction Hamiltonian is

$$\hat{H}_{\rm int}(t) = \frac{\lambda}{2}\hat{\sigma}_z \hat{X}(t) f(t,\tau), \tag{5}$$

where $\hat{X} = \hat{a} + \hat{a}^\dagger$ and $\hat{X}(t) = e^{i\hat{H}_{\rm osc}t}\hat{X}\, e^{-i\hat{H}_{\rm osc}t}$. We calculate the spin coherence, $\langle\hat{\sigma}_x(t)\rangle = \langle U^\dagger(t)\hat{\sigma}_x U(t)\rangle$, where the evolution operator is $\hat{U}(t) = \mathcal{T} e^{-\frac{i\lambda}{2}\hat{\sigma}_z\int_0^t dt'\hat{X}(t')f(t',\tau)}$ and $\mathcal{T}$ denotes time ordering. Since the interaction is proportional to $\hat{\sigma}_z$, it leads to pure dephasing and we obtain [22]

$$\langle\hat{\sigma}_x(t)\rangle = \left\langle \tilde{\mathcal{T}}\, e^{-i\hat{\phi}/2}\mathcal{T}\, e^{-i\hat{\phi}/2}\right\rangle_{\rm osc}, \tag{6}$$

where we used $\langle\hat{\sigma}_x(0)\rangle = 1$, the average $\langle\cdot\rangle_{\rm osc}$ is over oscillator degrees of freedom, $\tilde{\mathcal{T}}$ denotes anti-time ordering and the accumulated phase operator is

$$\hat{\phi} = \lambda\int_0^t dt'\hat{X}(t')f(t',\tau). \tag{7}$$

The spin coherence in equation (6) can be calculated using a cumulant expansion, which is vastly simplified by noting that the full Hamiltonian in equation (1), including the oscillator drive and ohmic dissipation, is quadratic in $\hat{X}$. As a result, the second cumulant—which, in general, corresponds to a Gaussian approximation—in the present case constitutes the exact result. We use this below to calculate the coherence for both thermal and driven motion.

Another consequence of the fact that $\hat{H}$ is quadratic in $\hat{X}$ is that the effect of the pulse sequence is completely characterized by its associated filter function [21, 23], $F(\omega\tau) = \frac{\omega^2}{2}|\tilde{f}(\omega)|^2$ with $\tilde{f}(\omega) = \int dt\, e^{i\omega t} f(t,\tau)$. The filter function describes how two-time position correlations $\left\langle\hat{X}(t)\hat{X}(t')\right\rangle$ of the oscillator affect the spin coherence in the second cumulant in the expansion of equation (6). For the pulse sequences illustrated in figure 1, the corresponding filter functions are

$$F(\omega\tau) = \begin{cases} 8\sin^4(\omega\tau/2), & \text{spin echo,} \\ 2\sin^2(N\omega\tau/2)\left[1-\sec(\omega\tau/2)\right]^2, & \text{CPMG.} \end{cases} \tag{8}$$

Note that phase-alternated versions of CPMG, such as XY4, which vary the axis of π pulse rotation in order to mitigate pulse errors, are also described by the above model in the limit of ideal pulses.

In practice, the average $\langle\sigma_x(t)\rangle$ is obtained by optically exciting the NV center and measuring its spin-dependent fluorescence. This optical readout is a source of noise that will be important in our discussion below. The contrast in fluorescence for an NV in $|m_s = 1\rangle$ compared to $|m_s = 0\rangle$ in current experiments is $(\alpha_0 - \alpha_1)/(\alpha_0 + \alpha_1) \sim 0.3$, where α_0 (α_1) is the average number of collected photons per measurement with the spin in state $|0\rangle$ ($|1\rangle$). After M measurements, the number of photons that discriminate between the 0 and 1 states is $M(\alpha_0 - \alpha_1)/2$, while the shot noise is $\sqrt{M(\alpha_0+\alpha_1)/2}$, resulting in the shot noise per measurement of $\sigma_{\rm shot} = \frac{\sqrt{2(\alpha_0+\alpha_1)/M}}{\alpha_0-\alpha_1}$. In addition, the spin projection noise per measurement is $\sigma_{\rm proj} = 1/\sqrt{M}$. Combining spin projection and shot noise assuming that they are independent results in the total noise per measurement, $\sigma_{\rm tot} = 1/K\sqrt{M}$, where $K = 1/\sqrt{1 + 2(\alpha_0+\alpha_1)/(\alpha_0-\alpha_1)^2}$ [21].

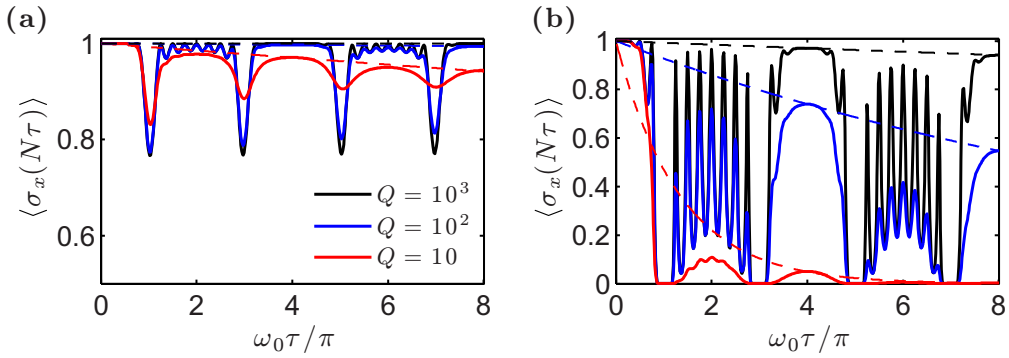

Figure 2. Spin coherence for CPMG sequence with $N = 8$, with an undriven thermal oscillator at temperature $T = 10\,\omega_0$ (a) and $T = 1000\,\omega_0$ (b) and the values of Q shown. Solid lines show full spin coherence with collapses and revivals, and dashed lines show oscillator-induced dephasing resulting in envelope decay given by equation (12). Here we took $\lambda/\omega_0 = 0.01$ and neglected intrinsic spin decoherence, $T_1 = T_2 \to \infty$.

2.3. Thermal motion

As discussed above, the spin coherence in equation (6) is given exactly by its second-order cumulant expansion. Since the total sequence time is $t = N\tau$, the coherence depends only on the time τ between π pulses,

$$\left\langle\hat{\sigma}_x(t = N\tau)\right\rangle = \mathrm{e}^{-\chi_N(\tau)}, \tag{9}$$

where

$$\chi_N(\tau) = \lambda^2 \int \frac{\mathrm{d}\omega}{2\pi} \frac{F(\omega\tau)}{\omega^2} \bar{S}_X(\omega), \tag{10}$$

and $\bar{S}_X(\omega) = \int \mathrm{d}t \mathrm{e}^{\mathrm{i}\omega t} \frac{1}{2}\langle\{\hat{X}(t), \hat{X}(0)\}\rangle$ is the symmetrized noise spectrum of $\hat{X}$. For the damped thermal oscillator described by $\hat{H}_{\mathrm{osc}}$ in the absence of a drive, the symmetrized spectrum is ($k_{\mathrm{B}} = 1$)

$$\bar{S}_X(\omega) = \frac{2\omega_0\gamma\omega\coth(\omega/2T)}{(\omega^2 - \omega_0^2)^2 + \gamma^2\omega^2}, \tag{11}$$

where $\gamma = \omega_0/Q$ is the mechanical damping rate due to coupling to the ohmic environment at temperature T.

We plot the spin coherence due to thermal motion in the classical limit $T \gg \omega_0$ in figure 2. The impact of the oscillator is greatest when the pulse sequence is synchronized with the cantilever frequency, $\tau = (2k+1)\pi/\omega_0$ with k an integer. At times $\tau = 2k\pi/\omega_0$, the accumulated phase due to the oscillator cancels within each free precession time, so that the accumulated phase variance averages nearly to zero and the coherence revives. We stress that this structure of collapse and revival can arise from purely classical motion; it is simply a consequence of averaging the phase variance accumulated by the spin over Gaussian-distributed magnetic field fluctuations with a characteristic frequency. In addition to collapses and revivals, the finite Q of the cantilever also causes dephasing of the spin, which leads to an exponential decay factor of the envelope as $\mathrm{e}^{-\Gamma_\phi\tau}$. In the limit $Q \gg 1$ and $T > \omega_0$, the dephasing rate is

given by

$$\Gamma_\phi \simeq 3N\eta^2\gamma\left(\bar{n}_{\rm th}+\frac{1}{2}\right), \tag{12}$$

where $\eta=\lambda/\omega_0$ is the dimensionless coupling strength and $\bar{n}_{\rm th}=(e^{\omega_0/T}-1)^{-1}$ is the thermal occupation number of the oscillator. We provide in the appendix a derivation of equation (12). Increasing Q not only increases the depth of the collapses in spin coherence due to the oscillator, but also decreases the overall spin dephasing, resulting in more complete revivals, as shown in figure 2. We also see that increasing the temperature increases both the depth of collapse and the dephasing. Below in section 3 we use these results to calculate the lowest temperature motion that can be detected, characterized by the phonon number sensitivity at the optimal pulse timing $\tau=\pi/\omega_0$.

2.4. Driven motion

It is straightforward to include the effects of a classical drive through $H_{\rm dr}$ in equation (1). This simply adds a classical deterministic contribution to $\hat{X}(t)$, and we can decompose the accumulated phase in equation (7) as $\hat{\phi}=\phi_{\rm dr}+\hat{\phi}_{\rm th}$, where

$$\phi_{\rm dr}=\lambda A\int {\rm d}t\,\cos\left(\omega_0 t+\theta_0\right) f(t,\tau) \tag{13}$$

is the classical accumulated phase due to the drive. Here, A is the dimensionless amplitude of driven motion and θ_0 is its phase at the start of a particular measurement. We assume that the cantilever drive is not phase-locked to the pulse sequence, so θ_0 is random and uniformly distributed between 0 and 2π. Using equation (6) and averaging over θ_0, we obtain

$$\left\langle\hat{\sigma}_x(t=N\tau)\right\rangle=J_0[a(\tau)]e^{-\chi_N(\tau)}, \tag{14}$$

where J_0 is the zeroth-order Bessel function [16], $a(\tau)=\eta A\sqrt{2F(\omega_0\tau)}$ and $\chi_N(\tau)$ is the thermal contribution given by equation (10). For a strong drive, thermal fluctuations are unimportant and the signal is given by the Bessel function. For a weak drive, comparable to thermal motion with $|A|^2\sim\bar{n}_{\rm th}$, both thermal and driven contributions may be important as illustrated in figure 3 and observed in experiment [13]. In figure 3, we see that, unlike thermal motion (see figure 2), driven motion can lead to dips in the spin coherence below zero. In the remainder of the paper, we focus on detecting thermal or quantum motion with the drive switched off.

3. Phonon number sensitivity

In this section we discuss the sensitivity limits of the spin used as a detector of undriven mechanical motion. By comparing the signal from thermal motion to the relevant noise sources, we obtain the phonon number sensitivity. We then discuss the sensitivity in several limits relevant to experiments.

3.1. Signal

The impact of an undriven thermal oscillator on the spin coherence in a spin echo or CPMG measurement sequence is described by equations (4) and (9). In addition to its coupling to the

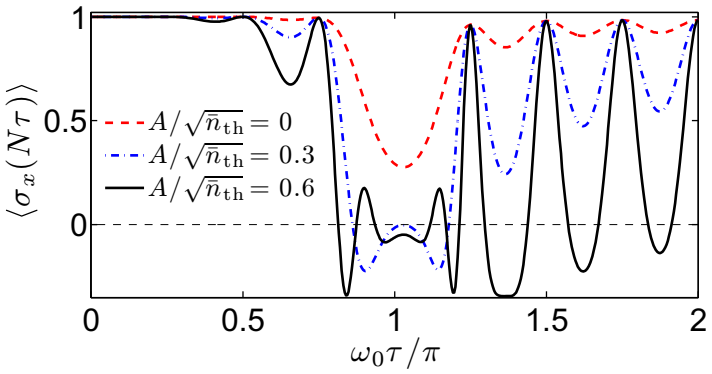

Figure 3. Spin coherence from combined thermal and driven motion for the drive amplitudes shown. For a weak drive, both driven and thermal contributions are important. The dips in the spin coherence below zero arise from driven motion, described by the Bessel function in equation (14). Parameters are $\omega_0/2\pi = 1\,\text{MHz}$, $T = 50\,\omega_0$, $Q = 100$.

oscillator, the spin is also coupled to an environment, which leads to intrinsic decoherence and degrades the signal. For an NV center, decoherence or T_2 processes are caused by a 1% natural abundance of ^{13}C nuclear spins in the otherwise ^{12}C lattice. Flip-flop processes between pairs of these nuclear spins produce low-frequency magnetic noise, which leads to decoherence of the form $e^{-N(\tau/T_2)^3}$ for a CPMG sequence with N pulses [21, 23]. Note that T_2 here refers to the decoherence time in a spin echo sequence (i.e. $N = 1$), typically $\sim$100 μs in natural diamond and up to $\sim$2 ms in isotopically pure diamond [24]. An added benefit of multipulse sequences is the enhanced spin coherence time, $\tilde{T}_2 = N^{2/3}T_2$, due to dynamical decoupling [14]. Finally, spin–lattice relaxation due to phonon processes leads to exponential decay on a timescale T_1, typically $\sim$1 ms at room temperature and up to $\sim$200 s at 10 K [25]. Including these intrinsic sources of spin decoherence, as well as the oscillator-induced decoherence Γ_ϕ given in equation (12), the probability of finding the spin in its initial state given in equation (4) is modified as

$$P(t = N\tau) = \frac{1}{2}\left(1 + e^{-N\left(\tau/T_1 + (\tau/T_2)^3\right)}e^{-\Gamma_\phi \tau}\right) - \mathcal{S}(\tau), \tag{15}$$

where we have isolated the coherent signal due to the oscillator,

$$\mathcal{S}(\tau) = \frac{1}{2}e^{-N\left(\tau/T_1 + (\tau/T_2)^3\right)}e^{-\Gamma_\phi \tau}\left(1 - e^{-\left(\chi_N(\tau) - \Gamma_\phi \tau\right)}\right). \tag{16}$$

Note that we have accounted for the oscillator-induced decoherence $\Gamma_\phi\tau$, which diminishes the coherent signal we are interested in.

We can obtain a simple analytic expression for the signal in the limit $Q \gg 1$. In this limit the oscillator spectrum is well approximated by Lorentzians at $\omega = \pm\omega_0$,

$$\bar{S}_X(\omega) \simeq \frac{\gamma\,(\bar{n}_{\rm th} + 1/2)}{(\omega - \omega_0)^2 + \gamma^2/4} + \frac{\gamma\,(\bar{n}_{\rm th} + 1/2)}{(\omega + \omega_0)^2 + \gamma^2/4}. \tag{17}$$

Using equation (17) with equation (10), we obtain a compact analytic expression for χ with no further approximation, which we provide in the appendix. We choose the pulse timing τ to maximize the impact of the oscillator motion on the spin coherence, providing optimal

sensitivity. This is achieved by setting $\tau = \pi/\omega_0$, flipping the spin every half-period of the oscillator and resulting in the maximum accumulated phase variance. For $N \gg 1$, the filter function with $\tau = \pi/\omega_0$ is well approximated by a Lorentzian centered at ω_0 of bandwidth $b\omega_0/N$, where $b \simeq 1.27$. Together with equation (17), this yields

$$\chi_N(\pi/\omega_0) \simeq \frac{16\eta^2 QN}{\pi\,(1+bQ/N)}\left(\bar{n}_{\rm th}+\frac{1}{2}\right), \tag{18}$$

and substituting this into equation (16), we obtain the signal.

3.2. Sensitivity

To find the sensitivity we must account for noise. As discussed in section 2.2, we combine spin projection and photon shot noise into a single parameter K so that the noise averaged over M measurements is $\sigma = 1/K\sqrt{M}$, where $M = t_{\rm tot}/N\tau$ is the number of measurements of duration $N\tau$ that can be carried out in a total time $t_{\rm tot}$. It follows that the minimum number of phonons that we can resolve in a given time $t_{\rm tot}$ is

$$\bar{n}_{\rm min} = \frac{\sigma}{|{\rm d}\mathcal{S}/{\rm d}\bar{n}_{\rm th}|}, \tag{19}$$

and the corresponding phonon number sensitivity is $\xi = \bar{n}_{\rm min}\sqrt{t_{\rm tot}}$. Using equations (16) and (18) with $\tau = \pi/\omega_0$, we obtain

$$\xi \simeq \frac{\pi^{3/2}}{8K\eta^2 QN}\,{\rm e}^{N/N_\phi}\left(1+\frac{bQ}{N}\right)\frac{1}{\sqrt{\omega_0/N}}, \tag{20}$$

where we have expressed the total spin dephasing in terms of a single pulse number,

$$N_\phi = \left[\frac{\pi}{\omega_0 T_1}+\left(\frac{\pi}{\omega_0 T_2}\right)^3+\frac{3\pi\eta^2}{Q}\left(\bar{n}_{\rm th}+\frac{1}{2}\right)\right]^{-1}, \tag{21}$$

which combines both intrinsic and oscillator-induced decoherence. Equations (20) and (21) reflect the competition between the oscillator damping rate $\gamma = \omega_0/Q$, the intrinsic decoherence times T_1 and T_2 of the spin and the measurement bandwidth $b\omega_0/N$. It is clear from equation (18) that increasing the number of pulses increases the coherent signal due to the oscillator; however, this also leads to increased spin decoherence. As a result, the resolvable phonon number is minimized at an optimal number of pulses,

$$N_{\rm opt} = N_\phi - bQ + \sqrt{N_\phi^2 + 6bQN_\phi + (bQ)^2}. \tag{22}$$

Note that the optimal pulse number is always set by the spin decoherence, $N_{\rm opt} \sim N_\phi$, with only a prefactor of the order of one depending on Q. Neglecting pulse imperfections, the optimized sensitivity is determined by an interplay of Q, T_1 and T_2 in equation (20). In practice, the optimal pulse number may be very large due to long spin coherence times, and pulse errors may play a role as discussed further below.

In figure 4 we plot the sensitivity as a function of pulse number N, and the optimized sensitivity as a function of coupling strength λ. To check the validity of the above approximations, it is straightforward to calculate the phonon number sensitivity directly from equations (10) and (11). The numerically exact sensitivity is shown in figure 4 in agreement with our analytic results. In the remainder of this section, we discuss the sensitivity in several experimentally relevant limits.

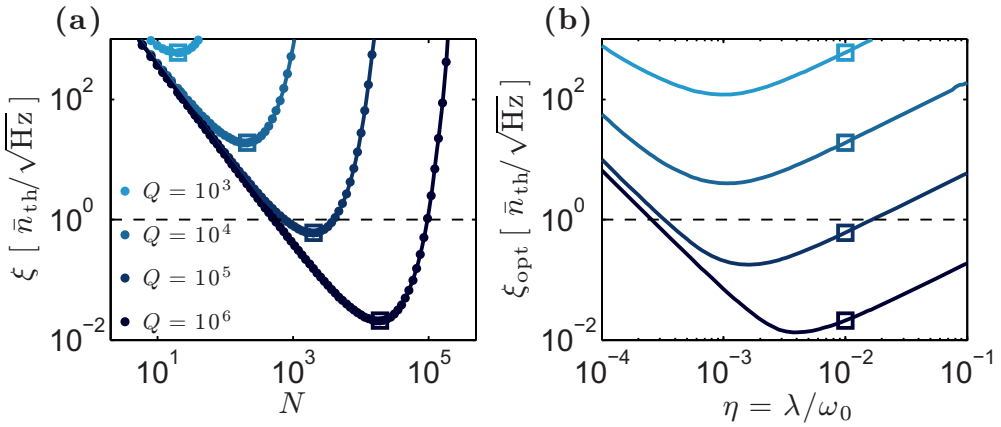

Figure 4. (a) Phonon number sensitivity ξ versus the number of pulses N for the values of Q shown and $\lambda/\omega_0 = 0.01$. Lines show the analytic result in equation (20) and points show the full numerical result using equations (10) and (11). Squares mark the sensitivity at the optimal pulse number $N_{\rm opt}$. (b) Sensitivity optimized with respect to N versus the coupling strength λ/ω_0 for the same values of Q as in (a). Squares mark the optimized sensitivity at $\lambda/\omega_0 = 0.01$, corresponding to the squares in (a). The dashed lines mark a sensitivity of $\xi = 1/\sqrt{\rm Hz}$. Parameters in both plots are $\omega_0/2\pi = 1\,{\rm MHz}$, $T_2 = 100\,\mu{\rm s}$, $T_1 = 100\,{\rm ms}$, $T = 4\,{\rm K}$ and $K = 0.3$.

3.3. Optimal sensitivity and cooperativity

An important limit for current experiments is one where the spin coherence is much longer than the oscillator coherence during the measurement, corresponding to $N_\phi > Q$. We assume that the spin coherence is dominated by intrinsic sources described by T_1 and T_2 and that the oscillator-induced spin decoherence Γ_ϕ can be neglected, well justified in the limit of weak coupling. Within these limits, the optimal number of pulses is $N_{\rm opt} \sim N_\phi$ and the optimized sensitivity is

$$\xi_{\rm opt} \simeq \frac{\pi^{3/2}}{8KC\sqrt{\omega_0/N_\phi}}, \tag{23}$$

where the cooperativity is

$$C = \frac{\lambda^2 \tilde{T}_2}{\gamma}, \tag{24}$$

and $\tilde{T}_2 = N_{\rm opt}^{2/3} T_2$ is the enhanced spin coherence time due to decoupling. For a large number of pulses, the enhanced spin coherence $N^{2/3}T_2$ may be very long, and ultimately the spin coherence may be limited by T_1 which is not suppressed by decoupling. In this case equations (23) and (24) are simply modified by $\tilde{T}_2 \to T_1$. The cooperativity parameter C is ubiquitous in quantum optics, and marks the onset of Purcell enhancement in cavity quantum electrodynamics. In the present case, $C > 1$ is the requirement for a single phonon to strongly influence the spin coherence, leading to a measurable signal despite the relatively short coherence time of the oscillator. The necessary condition $C > 1$ to resolve a single phonon can be simply understood: if the spin coherence is much longer than the oscillator coherence, i.e. $Q \ll N_\phi$, the accumulated phase

variance increases at a rate $\sim\lambda^2/\gamma$ (see equation (18) with sequence time $N\tau \sim N/\omega_0$) and the maximum interrogation time (assuming that oscillator-induced decoherence is negligible) is $\tilde{T}_2$. Note that we also require sufficiently low noise, characterized by K near one.

With feasible experimental parameters, $\tilde{T}_2 \sim T_1 \sim 10\,\text{ms}$, $\lambda/2\pi \sim 150\,\text{Hz}$, $\omega_0/2\pi \sim 1\,\text{MHz}$ and $Q \sim 1000$, a cooperativity of $C \sim 1$ can be reached. In current experiments, NV centers exhibit a 30% contrast in spin-dependent fluorescence, and collection efficiencies of 5% are realistic [21, 26]. These parameters yield $K \sim 0.3$ and an optimal phonon number sensitivity of $\xi_{\text{opt}} \sim 1/\sqrt{\text{Hz}}$ with $N \sim N_\phi \sim 15\,000$ pulses. Due to long spin coherence times T_1 and T_2, the optimal pulse number N_ϕ may be very large, and in practice finite pulse errors may play an important role in limiting the spin coherence. For example if the number of pulses is limited to $N \sim 1000$, a sensitivity of $\xi \sim 3/\sqrt{\text{Hz}}$ can be reached. We discuss this further below when we calculate the signal due to zero-point motion. Finally, we note that so far $\xi \sim 1$ only implies that our measurement device is, in principle, sensitive enough to detect mechanical position fluctuations corresponding to a few vibrational quanta. Below in section 4 we identify a modified requirement for resolving the zero-point motion in a realistic scenario, where an enhanced mechanical damping rate due to active ground state cooling is taken into account.

3.4. Ideal oscillators and ideal spin qubits

While the cooperativity regime describes an important part of parameter space, it is useful to briefly consider two more simple limits that describe the features in figure 4. First, we consider a harmonic oscillator that remains coherent for a much longer time than the entire pulse sequence, satisfying $Q \gg N$. In this limit, the long oscillator coherence time plays no role and the optimal sensitivity is limited only by the spin coherence, $\xi_{\text{opt}} \sim 1/(K\lambda^2\tilde{T}_2^2\sqrt{\omega_0/N})$. This limit can be seen on the left side of figure 4(a), where the sensitivities for different values of Q fall on the same curve at low pulse numbers N.

Finally, we consider the limit of very strong but incoherent coupling where the spin decoherence is dominated by the oscillator, i.e. Γ_ϕ becomes larger than $1/T_1$ and $1/T_2$. This limit is reached when either the intrinsic spin decoherence is negligible or for very strong coupling, $\eta^2\bar{n}_{\text{th}} \gg Q/(\omega_0 T_2)^3$, $Q/\omega_0 T_1$. In this limit, the coherent signal is large due to strong coupling, but saturates at a low number of pulses; further increasing the coupling strength only increases the oscillator-induced decoherence, reducing the signal. This is reflected in figure 4(b), where we see that increasing the coupling strength larger than $\eta^2 > 1/\gamma\bar{n}_{\text{th}}T_1$ no longer improves the optimized sensitivity but instead degrades it.

4. Detecting quantum motion

Above we found that for realistic experimental parameters, a single phonon can be resolved in 1 s of averaging time. This raises the intriguing question of whether a single spin can be used to sense the quantum zero-point motion of an oscillator in its ground state. It also implies that we must consider the effect of measurement backaction, which we have so far ignored in our discussion. To address these questions we analyze the experimentally relevant scenario where the spin is used to detect the motion of a mechanical resonator which is externally cooled close to its ground state.

4.1. Measuring a cooled oscillator

Even at cryogenic temperatures, a mechanical oscillator of frequency $\omega_0/2\pi \sim$ MHz has an equilibrium occupation number $\bar{n}_{\rm th}$ much larger than 1. For this reason we assume that the mechanical oscillator is cooled from its equilibrium occupation $\bar{n}_{\rm th}$ to a much lower value $\bar{n}_0 \sim 1$ using either optical cooling techniques [27] or the driven spin itself [8, 28]. An important consequence of cooling below the environmental temperature is the effective reduction in Q of the oscillator. For an oscillator coupled to both a thermal environment and an external, effective zero-temperature source for cooling, the mean phonon number satisfies

$$\langle \dot{n} \rangle = -(\gamma + \gamma_{\rm cool}) \langle n \rangle + \gamma \bar{n}_{\rm th}, \tag{25}$$

where $\gamma_{\rm cool}$ is the cooling rate. The steady-state occupation number is

$$\bar{n}_0 = \langle n \rangle \, (t \to \infty) = \frac{\gamma \bar{n}_{\rm th}}{\gamma + \gamma_{\rm cool}}, \tag{26}$$

and in order to maintain $\bar{n}_0 < 1$ we require that $\gamma_{\rm cool} > \gamma \bar{n}_{\rm th}$. As a result, the relevant decoherence rate of the oscillator is the rethermalization rate $\gamma \bar{n}_{\rm th}$. For this reason, to calculate the signal from a cooled oscillator we replace the equilibrium thermal occupation number $\bar{n}_{\rm th}$ by the effective occupation $\bar{n}_0 \to 0$ in all expressions, while at the same time replacing the intrinsic Q by the reduced, effective quality factor $Q_{\rm eff} = \omega_0/\gamma_{\rm cool} \approx Q/\bar{n}_{\rm th}$.

4.2. Single shot readout

In section 3 we calculated the sensitivity ξ, which reflects the minimum detectable phonon number $\bar{n}_{\rm min}$ that can be resolved in 1 s of averaging time. For the following discussion it is useful to convert the sensitivity to a minimum detectable phonon number per single measurement shot, $\bar{n}_{\rm min,1} = \xi/\sqrt{(N\pi/\omega_0)}$, where we have taken the total measurement time to be $t_{\rm tot} = N\tau$ and $\tau = \pi/\omega_0$. Assuming single shot spin readout ($K \to 1$), which has been demonstrated at low temperature [26], and using equation (20) we obtain

$$\bar{n}_{\rm min,1} = \frac{\pi \, {\rm e}^{N/N_\phi}}{8\eta^2 N Q_{\rm eff}} \left(1 + \frac{b Q_{\rm eff}}{N}\right) \sim \frac{1}{C_{\rm eff}}, \tag{27}$$

where $C_{\rm eff} = \lambda^2 \tilde{T}_2/\gamma \bar{n}_{\rm th}$ is the reduced, effective cooperativity. We see that under the assumption $N \sim N_{\rm opt} \gg Q_{\rm eff}$, the ability to resolve ground state fluctuations of a cooled oscillator within a few spin measurements requires $C_{\rm eff} > 1$, which is the same strong cooperativity condition required to perform a quantum gate between two spins mediated by a mechanical oscillator [19]. Alternatively, $\bar{n}_{\rm min,1}$ corresponds to the occupation number required to produce a signal $\mathcal{S}$ of the order of one in equation (16). It provides a convenient way to directly compare the sensitivity with the backaction due to sequential measurements, as discussed below.

In figure 5 we plot the calculated signal due to zero-point motion, assuming that the mechanical oscillator is cooled near its ground state $\bar{n}_0 = 0$ and using the reduced quality factor $Q_{\rm eff}$. These plots show that the intrinsic coherence times typical of NV centers are more than sufficient to resolve single phonons provided enough pulses can be applied to exploit the full spin coherence. In practice, the limiting factor is likely to be finite pulse errors, which limit the absolute number of pulses that can be applied before losing the spin coherence. To estimate the effect of finite pulse errors, we calculate the signal assuming additional spin decoherence

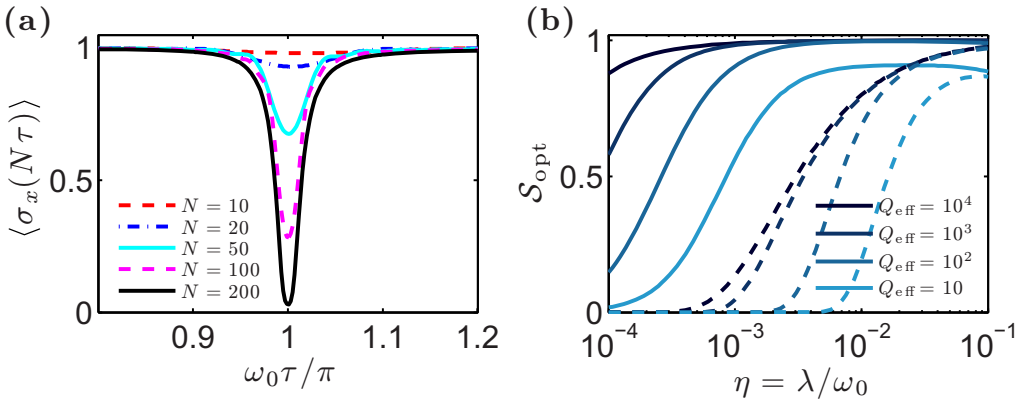

Figure 5. (a) Spin coherence with $\bar{n}_0 \sim 0$ for increasing pulse number and $Q_{\rm eff} = 100$ with $\lambda/\omega = 0.01$. (b) Optimal signal as defined in equation (16) from zero-point motion. Solid lines show optimal signal assuming an unlimited pulse number, while dashed lines include a simple treatment of pulse errors with $N_{\rm c} = 1000$ as described in the text. Parameters are $T_2 = 100\,\mu$s, $T_1 = 100$ ms, $\omega_0/2\pi = 1$ MHz.

of the form $e^{-N/N_{\rm c}}$ with a cutoff pulse number $N_{\rm c}$. Pulse numbers of $N \sim 160$ have been demonstrated in experiment [14], and with further improvements this can be increased to more than $N \sim 1000$. Based on this we plot the modified signal using $N_{\rm c} \sim 1000$ and find that even with a limited number of pulses, zero-point motion results in a significant signal for realistic coupling strengths.

4.3. Backaction

The result that a single spin magnetometer can resolve the quantum zero-point motion of a mechanical oscillator calls for a discussion of measurement backaction. We begin by noting that, despite the linear coupling of the spin to the oscillator position in equation (1), the described measurement protocol is sensitive to the *variance* of the accumulated phase $\sim\langle\hat{X}^2\rangle$, which we obtain by averaging independent spin measurements. As a result, our approach does not correspond to standard continuous position measurement [29], nor does it implement a quantum nondemolition measurement of the phonon number, since the interaction in equation (1) does not commute with $\hat{n}$. In principle, by cooling between measurements our approach may be used to measure the phonon number with arbitrary precision. This justifies our discussion of the sensitivity neglecting the backaction, presented in section 3. Nonetheless, the effect of the spin's backaction on the oscillator is both a practical issue and interesting in itself, and could be used to prepare nonclassical mechanical states. We describe two possible approaches to observe the influence of measurement backaction on the oscillator.

First, we consider probing directly the projective nature of the measurement. For simplicity, we assume that the oscillator is initially in its ground state and decoupled from the environment, and assume single shot spin readout. In a single measurement sequence, the oscillator experiences a spin-dependent force according to equation (5). Measuring $\langle\hat{\sigma}_x\rangle = \pm 1$ at the end

of the sequence projects the oscillator onto a superposition of coherent states [6, 30],

$$|\psi_{\pm}\rangle = \frac{|\mathrm{i}\,\alpha\rangle \pm |-\mathrm{i}\,\alpha\rangle}{\sqrt{2 \pm 2\,\mathrm{e}^{-2\alpha^2}}}, \tag{28}$$

where $\alpha = N\lambda/2\omega_0$ is the total displacement for a sequence of $N \gg 1$ pulses and $\tau = \pi/\omega_0$. The probabilities to measure $|\pm\rangle$ are given by

$$p_{\pm} = \frac{1}{2}\left(1 \pm \mathrm{e}^{-2\alpha^2}\right), \tag{29}$$

which shows, consistent with the above discussion, that for a measurement strength $\alpha > 1$ the oscillator in its ground state can significantly affect the spin dynamics. To observe the backaction of this measurement on the oscillator, we can carry out a second spin measurement, which is sensitive to the state of the oscillator conditioned on the first measurement. In principle, by using techniques developed in cavity quantum electrodynamics, this procedure can be used to fully reconstruct the conditionally prepared oscillator state [31]. However, this requires very strong coupling $\lambda > \gamma\bar{n}_{\mathrm{th}}$, making direct observation of projective backaction more challenging than resolving zero-point motion.

Let us now consider an alternative, indirect way to observe backaction by making many successive measurements. Again beginning with the oscillator near its ground state, the first measurement projects the oscillator into one of the states $|\psi_{\pm}\rangle$. By averaging over the two possible spin measurement outcomes, the resulting mixed oscillator state is

$$\rho_{\mathrm{osc}} = p_+ |\psi_+\rangle \langle\psi_+| + p_- |\psi_-\rangle \langle\psi_-|, \tag{30}$$

and we see that on average the oscillator energy has increased by $|\alpha|^2$. Repeating this measurement many times, without cooling between measurements, the oscillator amplitude undergoes a random walk of step size $\pm\alpha$, and on average the phonon number increases approximately linearly in time. This corresponds to backaction heating described by an effective diffusion rate,

$$D_{\mathrm{ba}} = \frac{N\eta^2\omega_0}{4\pi}. \tag{31}$$

Combining the measurement backaction with intrinsic mechanical dissipation and external cooling, the average occupation number satisfies

$$\langle\dot{n}\rangle = -(\gamma + \gamma_{\mathrm{cool}})\langle n\rangle + \gamma\bar{n}_{\mathrm{th}} + D_{\mathrm{ba}}, \tag{32}$$

and for $\gamma_{\mathrm{cool}} \gg \gamma$ the steady-state phonon number added due to backaction is

$$\bar{n}_{\mathrm{ba}} = \frac{D_{\mathrm{ba}}}{\gamma_{\mathrm{cool}}} = \frac{NQ_{\mathrm{eff}}\eta^2}{4\pi}. \tag{33}$$

We see that increasing the coupling strength not only improves the single shot resolution $\bar{n}_{\mathrm{min},1}$, but also leads to backaction heating of the oscillator. For sufficiently strong coupling, the steady-state backaction phonon number $\bar{n}_{\mathrm{ba}}$ exceeds the phonon number resolution, and the inferred phonon number is determined by backaction. We thus take the sum $\bar{n}_{\mathrm{meas}} = \bar{n}_{\mathrm{min},1} + \bar{n}_{\mathrm{ba}}$ as a measure of the minimum inferred phonon number. Note that for simplicity in this discussion we have assumed the limit $N \ll Q_{\mathrm{eff}}$, in which the oscillator is coherent within each measurement sequence. Within this limit we find that

$$\bar{n}_{\mathrm{meas}} = \frac{\pi\alpha}{8\eta^2N^2} + \frac{NQ_{\mathrm{eff}}\eta^2}{4\pi}. \tag{34}$$

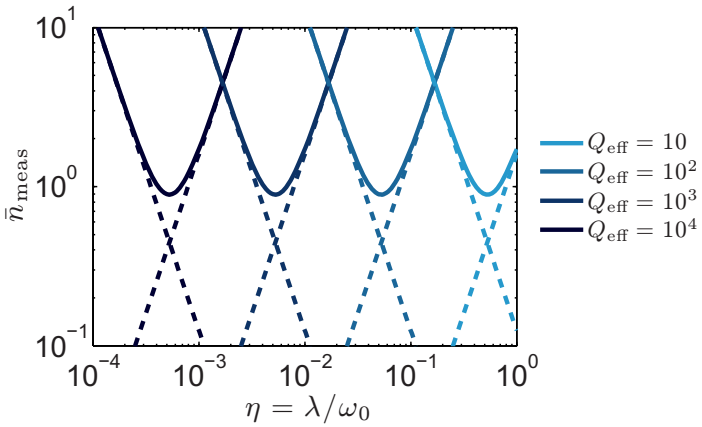

Figure 6. Solid lines show the total inferred phonon number given by equation (33) from combined phonon resolution and backaction heating. Dashed lines show sensitivity and heating contributions. For each value of $Q_{\rm eff}$ we set $N = Q_{\rm eff}/5$.

The total inferred phonon number $\bar{n}_{\rm meas}$ is shown in figure 6 as a function of the coupling parameter η and a fixed number of pulses $N = Q_{\rm eff}/5$. In this case $\bar{n}_{\rm meas}$ is minimized for $\eta \sim 1/\sqrt{Q_{\rm eff}}$, where it reaches a value of $\bar{n}_{\rm meas} \sim \mathcal{O}(1)$. Observing this minimum in the phonon number resolution as a function of coupling strength would provide an indirect signature of measurement backaction. This observation may be more feasible in near-term experiments than directly observing projective backaction as discussed above.

5. Summary and conclusions

We have presented the sensitivity limits of a novel position sensor consisting of a single spin. For realistic experimental parameters, we predict that a single NV center in diamond can be used to resolve single phonons in a cooled, magnetized mechanical cantilever. The condition to resolve single phonons is that of strong effective cooperativity, the same condition needed to perform a quantum gate between two spins mediated by a mechanical oscillator. For even stronger coupling, the backaction of the spin on the oscillator can be probed directly or indirectly, and used to prepare nonclassical mechanical states.

Acknowledgments

This work was supported by the NSF, CUA, DARPA and the Packard Foundation. SDB acknowledges support from the NSERC of Canada and ITAMP. SK acknowledges support from the DoD through the NDSEG program and the NSF through the NSFGRP under grant no. DGE-1144152. QPU acknowledges support from the Deutschen Forschungsgemeinschaft. PR acknowledges support from the Austrian Science Fund (FWF) through SFB FOQUS and START grant no. Y 591-N16.

Appendix. Analytic signal for thermal motion in the high-*Q* limit

Here we sketch the derivation of equations (12) and (18). The impact of the oscillator on the spin coherence is given by equations (10) and (11),

$$\chi_N(\tau) = 2\omega_0\gamma\lambda^2 \int \frac{\mathrm{d}\omega}{2\pi} \frac{F(\omega\tau)}{\omega^2} \frac{\omega \coth(\omega/2T)}{(\omega^2-\omega_0^2)^2+\gamma^2\omega^2}. \tag{A.1}$$

To perform this integral it is useful to decompose the filter function as

$$F(\omega\tau) = 1-\cos(N\omega\tau) + \sum_{j=0}^{N-1}(-1)^j\Big[\big(1-\cos(\omega s_j)\big) - j\,\big(1-\cos(\omega t_j)\big)\Big], \tag{A.2}$$

where $s_j = (j+1/2)\tau$ and $t_j = (N-j)\tau$. We first consider the high-temperature limit, $T \gg \omega_0$, in which we can approximate $\coth(\omega/2T) \approx 2T/\omega$. The result is a sum of integrals of the form

$$4\,T\omega_0\gamma\lambda^2 \int \frac{\mathrm{d}\omega}{2\pi} \frac{1-\cos(\omega t)}{\omega^2\left[(\omega^2-\omega_0^2)^2+\gamma^2\omega^2\right]} = \eta^2(2\bar{n}_{\mathrm{th}})q(t), \tag{A.3}$$

which can be done exactly. In the limit $Q \gg 1$ we obtain that

$$q(t) = \gamma t + \big(1-\mathrm{e}^{-\gamma t/2}\cos(\omega_0 t)\big) - \frac{4\gamma}{3\omega_0}\,\mathrm{e}^{-\gamma t/2}\sin(\omega_0 t). \tag{A.4}$$

To calculate Γ_ϕ we need the spin coherence at the revivals, given by $\chi_N(\tau = 4\pi/\omega_0)$. To first order in γt, we have $q(t = 4\pi/\omega_0) \simeq 3\gamma t/2$, and to this order the only nonzero term in equation (A.1) is due to the $1-\cos(N\omega\tau)$ terms in equation (A.2). The result is equation (12).

Next we derive equation (18) at $\tau = \pi/\omega_0$ in the limit $N \gg 1$. Here we use the fact that the filter function near $\tau \simeq \pi/\omega_0$ may be rewritten for $N \gg 1$ as $F(\omega\pi/\omega_0) \simeq 2N^2\,\mathrm{sinc}^2\,[\pi N(\omega-\omega_0)/2]$, and in turn this function is well approximated by its Lorentzian envelope

$$F(\omega\pi/\omega_0) \simeq \frac{(b\omega_0)^2/2}{(\omega-\omega_0)^2+(b\omega_0/N)^2/4}, \tag{A.5}$$

where we obtain the effective bandwidth $b\omega_0/N$ by fitting the filter function to the form of equation (A.5), which yields $b \simeq 1.27$. At the collapse time $\tau = \pi/\omega_0$, we can approximate $\bar{S}_X(\omega)$ by the Lorentzian spectrum given in equation (17). Using equations (17) and (A.5), $\chi(\pi/\omega_0)$, the integrand is simply the product of two Lorentzians and performing the integration yields equation (18).

References

[1] LaHaye M D, Suh J, Echternach P M, Schwab K C and Roukes M L 2009 *Nature* **459** 960–4
[2] O'Connell A D *et al* 2010 *Nature* **464** 697
[3] Armour A D, Blencowe M P and Schwab K C 2002 *Phys. Rev. Lett.* **88** 148301
[4] Rugar D, Budakian R, Mamin H J and Chui B W 2004 *Nature* **430** 329
[5] Treutlein P, Hunger D, Camerer S, Haensch T W and Reichel J 2007 *Phys. Rev. Lett.* **99** 140403
[6] Steinke S K, Singh S, Tasgin M E, Meystre P, Schwab K C and Vengalattore M 2011 *Phys. Rev.* A **84** 023841
[7] Gullo N, Busch T, Palma G and Paternostro M 2011 *Phys. Rev.* A **84** 063815
[8] Rabl P, Cappellaro P, Dutt M V G, Jiang L, Maze J R and Lukin M D 2009 *Phys. Rev.* B **79** 041302

[9] Pályi A, Struck P R, Rudner M S, Flensberg K and Burkard G 2012 *Phys. Rev. Lett.* **108** 206811
[10] Balasubramanian G *et al* 2008 *Nature* **455** 648
[11] Hong S, Grinolds M S, Maletinsky P, Walsworth R L, Lukin M D and Yacoby A 2012 *Nano Lett.* **12** 3920
[12] Arcizet O, Jacques V, Siria A, Poncharal P, Vincent P and Seidelin S 2011 *Nature Phys.* **7** 879
[13] Kolkowitz S, Bleszynski Jayich A C, Unterreithmeier Q P, Bennett S D, Rabl P, Harris J G E and Lukin M D 2012 *Science* **335** 1603
[14] de Lange G, Wang Z H, Ristè D, Dobrovitski V V and Hanson R 2010 *Science* **330** 60
[15] Maze J R *et al* 2008 *Nature* **455** 644
[16] de Lange G, Ristè D, Dobrovitski V V and Hanson R 2011 *Phys. Rev. Lett.* **106** 080802
[17] Naydenov B, Dolde F, Hall L T, Shin C, Fedder H, Hollenberg L C L, Jelezko F and Wrachtrup J 2011 *Phys. Rev.* B **83** 081201
[18] Laraoui A, Hodges J S and Meriles C A 2010 *Appl. Phys. Lett.* **97** 143104
[19] Rabl P, Kolkowitz S J, Koppens F H L, Harris J G E, Zoller P and Lukin M D 2010 *Nature Phys.* **6** 602
[20] Armour A D and Blencowe M P 2008 *New J. Phys.* **10** 095004
[21] Taylor J M, Cappellaro P, Childress L, Jiang L, Budker D, Hemmer P R, Yacoby A, Walsworth R L and Lukin M D 2008 *Nature Phys.* **4** 810
[22] Makhlin Y and Shnirman A 2004 *Phys. Rev. Lett.* **92** 178301
[23] de Sousa R 2009 *Top. Appl. Phys.* **115** 183
[24] Balasubramanian G *et al* 2009 *Nature Mater.* **8** 383
[25] Jarmola A, Acosta V M, Jensen K, Chemerisov S and Budker D 2012 *Phys. Rev. Lett.* **108** 197601
[26] Robledo L, Childress L, Bernien H, Hensen B, Alkemade P F A and Hanson R 2011 *Nature* **477** 574
[27] Marquardt F, Chen J, Clerk A A and Girvin S 2007 *Phys. Rev. Lett.* **99** 093902
[28] Rabl P 2010 *Phys. Rev.* B **82** 165320
[29] Caves C M, Thorne K, Drever R, Sandberg V and Zimmermann M 1980 *Rev. Mod. Phys.* **52** 341
[30] Tian L 2005 *Phys. Rev.* B **72** 195411
[31] Deleglise S, Dotsenko I, Sayrin C, Bernu J, Brune M, Raimond J M and Haroche S 2008 *Nature* **455** 510